Published in final edited form as:
Alzheimer Dis Assoc Disord. 2012 January ; 26(1): 8–16. doi:10.1097/WAD.0b013e31821300bc.

Correlation of amyloid PET ligand florbetapir F 18 (^{18}F-AV-45) binding with β-amyloid aggregation and neuritic plaque deposition in postmortem brain tissue

Seok Rye Choi[1], **Julie A. Schneider**[2,3], **David A. Bennett**[3], **Thomas G. Beach**[4], **Barry J. Bedell**[5,6], **Simone P. Zehntner**[5], **Michael Krautkramer**[1], **Hank F. Kung**[7,8,9], **Daniel M. Skovronsky**[1,7], **Franz Hefti**[1], and **Christopher M. Clark**[1,9]

[1] Avid Radiopharmaceutical Inc., Philadelphia, PA 19104

[2] Department of Pathology, Rush Alzheimer's Disease Center, Rush University Medical Center, Chicago IL

[3] Department of Neurological Sciences, Rush Alzheimer's Disease Center, Rush University Medical Center, Chicago IL

[4] Civin Laboratory for Neuropathology, Banner Sun Health Research Institute, Sun City, AZ

[5] Biospective Inc, Montreal, Quebec, Canada

[6] Montreal Neurological Institute, McGill University, Montreal, Quebec, Canada

[7] Department of Radiology, University of Pennsylvania, Philadelphia, PA 19104

[8] Department of Pharmacology, University of Pennsylvania, Philadelphia, PA 19104

[9] Department of Neurology, University of Pennsylvania, Philadelphia, PA 19104

Abstract

Background—Florbetapir F 18 (^{18}F-AV-45) is a positron emission tomography (PET) imaging ligand for the detection of amyloid aggregation associated with Alzheimer's disease. Earlier data showed that florbetapir F 18 binds with high affinity to β-amyloid plaques in human brain homogenates (Kd = 3.7 nM) and has favorable imaging pharmacokinetic properties, including rapid brain penetration and washout. The present study used human autopsy brain tissue to evaluate the correlation between *in vitro* florbetapir F 18 binding and β-amyloid density measured by established neuropathological methods.

Methods—The localization and density of florbetapir F 18 binding in frozen and formalin-fixed paraffin-embedded sections of postmortem brain tissue from 40 subjects with a varying degree of neurodegenerative pathology was assessed by standard florbetapir F 18 autoradiography and correlated with the localization and density of β-amyloid identified by silver staining, thioflavin S staining, and immunohistochemistry.

Corresponding author contact information: Christopher M. Clark, Avid Radiopharmaceuticals, Inc., 3711 Market Street, 7th Floor, Philadelphia, PA 19104, USA, 215.298.0725, Clark@avidrp.com.

Contributions: S-R. Choi performed the majority of experiments; J. A. Schneider and T. G. Beach performed neuropathological examinations, selected and provided appropriate human tissue material and conducted the histochemical amyloid load estimates. D. Bennett supervised the histologic and IHC studies done at Rush University. B. J. Bedell, and S. P. Zehntner performed some of the quantitative IHC studies, S-R. Choi, F. Hefti, and C.M. Clarkwrote the paper with the assistance of the other authors, M. Krautkramer participated in the design and logistics of the study, D. M. Skovronsky, C.M. Clark, F. Hefti, and H. Kung participated in the planning of the study and review of the data.

Results—There were strong quantitative correlations between florbetapir F 18 tissue binding and both β-amyloid plaques identified by light microscopy (sliver staining and thioflavin S fluorescence) and by immunohistochemical measurements of β-amyloid using three antibodies recognizing different epitopes of the β-amyloid peptide (Aβ). Florbetapir F 18 did not bind to neurofibrillary tangles.

Conclusion—Florbetapir F 18 selectively binds β-amyloid in human brain tissue. The binding intensity was quantitatively correlated with the density of β-amyloid plaques identified by standard neuropathological techniques and correlated with the density of Aβ measured by immunohistochemistry. Since β-amyloid plaques are a defining neuropathological feature for Alzheimer's disease, these results support the use of florbetapir F 18 as an amyloid PET ligand to identify the presence of AD pathology in patients with signs and symptoms of progressive late-life cognitive impairment.

Keywords

PET imaging; Alzheimer's disease; β-amyloid plaque; autoradiography; β-amyloid; amyloid PET imaging; florbetapir F 18; ^{18}F-AV-45; postmortem

INTRODUCTION

Alzheimer's disease (AD) pathology is thought to begin years before the first clinical manifestations of brain failure. The inability to directly identify the pathological changes in living persons and the overlap of signs and symptoms associated with different late-life neurodegenerative dementing diseases adds a measure of uncertainty to the clinical diagnosis of AD in individual patients. The inclusion of pathologically-linked biomarkers in the clinical evaluation of patients with progressive late-life cognitive impairment should improve clinical diagnostic accuracy[1, 2].

The presence of β-amyloid plaques (Aβ plaque) is a defining neuropathological feature of AD.[3–6] A definitive diagnosis of AD requires both progressive dementia and histopathologic demonstration in the neocortex of neuritic plaques, consisting primarily of aggregated β-amyloid, and neurofibrillary tangles composed of aggregates of hyperphosphorylated tau protein. PET imaging of β-amyloid aggregates in the brains of patients with signs and symptoms of progressive late-life cognitive impairment will provide a new clinical tool for the direct identification of amyloid pathology, facilitating an accurate clinical diagnosis.

Several radioactively labeled molecules have been identified as potentially useful PET ligands to visualize β–amyloid aggregates. The most widely studied ligand is ^{11}C-labeled Pittsburgh compound B (^{11}C-PiB), a thioflavin T derivative. Preclinical and clinical studies suggest that ^{11}C-PiB binds with high affinity and selectivity to amyloid aggregates in the brain.[7–9] However, the 20 minute half-life of ^{11}C limits its use in routine clinical care and has triggered the search for ^{18}F- ligands. Three ^{18}F- ligands are currently in active development: florbetapir F 18 (^{18}F-AV-45, Avid), florbetaben F 18 (BAY 94-9172, Bayer-Schering);[10] and flutemetamol F 18, (GE067, General Electric)[11].

Early data showed that florbetapir F 18 binds with high affinity to β-amyloid plaques in human brain homogenates (Kd = 3.7 nM) and has desirable brain imaging pharmacokinetic properties, including rapid brain penetration and washout.[12–14] Initial in vitro autoradiography studies showed that florbetapir F 18 bound with high affinity to β-amyloid deposits in tissue sections from brains of patients with AD, whereas no signal was observed in tissue sections from control subjects.[12]

The objectives of the study were to validate the ability of florbetapir F 18 to accurately identify and quantify amyloid aggregates in human autopsy tissue by (1) determining the relationship between florbetapir F 18 tissue retention as measured by autoradiography (ARG) and the localization of amyloid plaques using double-labeling studies, and (2) determining the correlation between the intensity of the ligand signal (florbetapir F 18 binding by Bmax or ARG optical density) and β-amyloid deposition using state-of-the-art neuropathologic methods.

METHODS

Autoradiography

Florbetapir F 18 autoradiography was performed on sections of postmortem human brain tissue from 40 older subjects with and without AD or other age-related pathologies. We included 24 cases from the Religious Orders Study of the Rush Alzheimer's Disease Center at Rush University, Chicago, IL (Rush ADC) selected to ensure representation of a spectrum of AD pathology[15] and 16 from the Banner Sun Health Research Institute Brain Donation Program, Sun City, AZ (BSHRI)[16] chosen to represent a range of pathologic diagnoses including 2 subjects free of pathology, 7 subjects with AD, 3 subjects with vascular dementia and 4 subjects with progressive supranuclear palsy.

Autopsy procedures from both studies have been previously described.[15, 16] Briefly, tissue from the frontal cortex was fixed in 4% paraformaldehyde, embedded in paraffin, and cut to prepare 6 μm (Rush ADC) sections. In addition, frozen tissue was available from the 16 of the BSHRI cases. The florbetapir F 18 autoradiography and β-amyloid binding (Bmax binding), as well as the double labeling studies, were performed at Avid Radiopharmaceuticals.

In vitro florbetapir F 18 autoradiography and double labeling

Florbetapir F 18 was synthesized as previously described[12] and incubated with the brain tissue sections. After drying, the sections were exposed to Kodak Biomax MR film for 12–18 hours. The images were digitized and the optical density (OD) of the signal in the gray matter determined.

To evaluate the co-localization of florbetapir F 18 binding with neuritic plaques, double labeling of autoradiography and thioflavin S fluoromicroscopy was performed in sections from the same tissue blocks used for the silver and immunohistochemistry staining.

Following incubation with florbetapir F 18, the 6 μm sections were immersed in 10% neutral buffered formalin for 1 hour, treated with 0.05% $KMnO_4$ followed by 0.2% $K_2S_2O_5$/0.2% oxalic acid for quenching of autofluorescence, and stained with 0.025% thioflavin S. The density of fluorescence-positive neuritic plaques was evaluated visually under the microscope using a semi-quantitative scoring of 0 (none), 1 (sparse), 2 (moderate), and 3 (frequent).

Semi-quantitative measures of β-amyloid plaques and neurofibrillary tangles

Neuritic and diffuse β-amyloid plaques and neurofibrillary tangles from the 24 Rush ADC subjects were identified on 6 μm sections using a modified Bielschowsky sliver stain.[17] The density of each of the three pathologies was determined by counting the number of each in a 1 square mm area (X100 magnification) in the region with greatest density for that particular measure, and then assigning a 6-level semi-quantitative score of 0 (none) to 5 (frequent), based on these counts.

For the 16 BSHRI cases, a Campbell-Switzer silver stain was used to identify β-amyloid plaques and a Gallyas silver stain to identify neurofibrillary tangles. A semi-quantitative score ranging from 0 (none) to 3 (very dense) in quarter-point increments was used to assess plaque and tangle density. All plaque types (i.e. neuritic and diffuse) were included in the plaque score.

The neuropathological assessment was performed by experts blinded to the results of florbetapir F 18 autoradiography, thioflavin-S staining, and β-amyloid tissue binding (Bmax) results.

Quantitative measures of β-amyloid aggregation by image analysis

The density of β-amyloid was quantified using three different antibodies, namely 10D5, a monoclonal mouse anti-human β-amyloid antibody, that recognizes the N-terminal of the β-amyloid peptide[18] (courtesy of Elan Pharmaceuticals, South San Francisco, CA); 6F/3D, a monoclonal mouse anti-human β-amyloid antibody, that recognizes an epitope near the N-terminus of the β-amyloid peptide[19, 20] (Dako North America; Carpinteria, CA); and 4G8, a monoclonal anti-human β-amyloid antibody that recognizes an epitope generated by amino acids 17–24 in the middle of the human β-amyloid peptide[21, 22] (Covance, Princeton NJ). The immunohistochemistry (IHC) studies were performed on sections adjacent to those used for silver staining and autoradiography.

For studies using 10D5 (dilution 1:300) and 6F/3D (dilution 1:50), tissue samples from the 24 Rush ADC subjects were stained using an Automated Leica Bond Immunostainer (Leica Microsystems Inc., Bannockborn IL). An investigator blinded to the clinical and pathologic data, outlined the cortical gray region of interest on each slide using a Microbrightfield Stereology System. The Stereo Investigator 8.0 software program (MicroBrightField, Inc., Williston, VT) was used to place a 1300 × 1030 μm grid over the region and 200X images were captured at interval grid intersection points. Area analysis was performed using Image J 1.42g (http://rsbweb.nih.gov/ij/) which segmented each image along the intensity domain into two fractions, the labeled (amyloid) and the background compartment. The mean fraction of β-amyloid per region and per subject was computed, yielding a value for the area occupied by amyloid. Data from two adjacent blocks of tissue (1 cm apart) were averaged to obtain a composite measure of the percent area occupied by β-amyloid in each region of interest. 10D5 and 6F/3D IHC were performed on adjacent sections from the same block.

The 4G8 antibody studies were performed using sections cut from two tissue blocks taken from the frontal lobe of 21 of 24 Rush ADC cases (tissue for IHC from both blocks was not available for 3 cases). Deparaffinized and rehydrated 6 μm thick tissue sections underwent formic acid-induced antigen-retrieval, and were incubated with the anti-Aβ antibody 4G8 (Covance; dilution 1:2000, 90 minutes) and subsequently visualized with anti-rabbit biotin-streptavidin horseradish peroxidase (HRP) and AEC chromogen. The sections were counterstained with Acid Blue 129 and coverslipped using an aqueous mounting media.[23] The stained slides were digitized using a Zeiss MIRAX high-resolution, automated slide scanner (Carl Zeiss Canada, Toronto, ON) and the digital images were converted from MIRAX to MINC (Medical NetCDF) file format. Image quantification was performed using the PERMITS™ image processing/analysis software (Biospective Inc., Montreal, Canada). This automated quantification method segments chromogen-positive pixels based on RGB intensity and generates a parametric map of beta-amyloid burden over the entire tissue section. The amyloid burden (% area) was then calculated for the gray matter (*i.e.* cortex) and white matter for each tissue section.

Florbetapir F 18 binding in tissue homogenates

The methods used to evaluate the binding of florbetapir F 18 to brain tissue homogenates are described in detail elsewhere.[12] Briefly, using frozen tissue from the 16 BSHRI cases gray matter was homogenized and saturation binding assays carried out using BTA-1 (8 μM) to define non-specific binding.

RESULTS

Co-localization of florbetapir F 18 autoradiography and amyloid plaques

There was good co-localization of the florbetapir autoradiography signal with thioflavin S-positive neuritic plaque structures when tissue sections from formalin-fixed, paraffin-embedded tissue sections from AD patients were double-labeled with florbetapir F 18 (figure 1).

Correlation of florbetapir F 18 binding with β-amyloid plaques and neurofibrillary tangles

Florbetapir F 18 autoradiography (ARG) demonstrated a broad spectrum of signal intensities in the 16 BSHRI tissue samples. Representative ARG images are shown in figure 2. The density of florbetapir F 18 binding was quantified by optical measurements of the autoradiographic signal and compared to the maximal specific binding (Bmax) in homogenates of tissue adjacent to the autoradiography sections (table 1). There was a strong ($r = 0.95$) correlation between the density of the autoradiographic signal and its maximal specific binding (Bmax) to amyloid aggregates in the brain homogenates (table 2).

In addition, total plaques scores (BSHRI method) in these 16 cases correlated with both the Bmax of florbetapir F 18 binding in tissue homogenates ($r = 0.88$) and the optical density of the autoradiography signal ($r = 0.95$) (table 2). In contrast, neurofibrillary tangle scores were not significantly associated with florbetapir F 18 binding ($r = 0.33$, $p = 0.21$)

The relationship between florbetapir F 18 ARG binding and plaque score was explored further using postmortem brain tissue from the 24 Rush University cases. These samples also had various degrees of amyloid plaque pathology as determined by silver staining. As seen with the BSHRI cases, there were strong correlations between the florbetapir F 18 autoradiographic signal intensity and semi-quantitative plaque density identified by both Bielschowsky silver and thioflavin S with Spearman's rank correlation coefficient values of 0.71 and 0.81, respectively (table 3).

Correlation of florbetapir F 18 binding and quantitative measures of β-amyloid aggregation

We compared the immunohistochemistry values (average of two areas from the frontal lobe of each subject) for each of the three amyloid antibodies with the florbetapir F 18 autoradiography average value from the same two areas. Figure 3 shows representative examples of immunohistochemical staining for each antibody. The correlation coefficients and p-values comparing florbetapir F 18 autoradiography with β-amyloid density measured by 6F/3D, 4G8, and 10D5, as well as by Bielschowsky silver staining and thioflavin S fluorescence are presented in table 3. Figure 4 shows the 4G8 β-amyloid immunostaining and the florbetapir F 18 autoradiography of adjacent sections. A comparison of the immunohistochemistry quantification and florbetapir F 18 autoradiographical density for each of the 21 tissue samples is shown in table 4. All three β-amyloid antibodies correlated well with florbetapir F 18, yielding correlation coefficients between 0.75 and 0.88. There was also an excellent correlation among the three antibodies. These data are plotted (figure 5).

DISCUSSION

The addition of pathologically-linked biomarkers to the assessment of patients with progressive late-life cognitive impairment will likely improve the validity of a clinical diagnosis of AD made at the earliest symptomatic stage. These studies represent the first documentation of the correlation between a florbetapir F 18 autoradiography signal and the microscopic and immunohistochemistry quantification of β-amyloid, including plaque pathology, in human autopsy tissue. The data supports the following conclusions: 1) there is a strong correlation between the density of in vitro florbetapir F 18 binding in human autopsy tissue semi-quantitative estimates of β-amyloid plaque density as determined by both silver and thioflavin S stains; 2) there is an equally strong correlation between the density of in vitro florbetapir F 18 binding and the density of β-amyloid as determined by image analysis of immunostained brain sections using three different β-amyloid antibodies; 3) the intensity of the florbetapir F 18 autoradiography signal in human autopsy sections is correlated with the degree of ligand binding in regional brain homogenates; and 4) florbetapir F 18 does not bind to neurofibrillary tangles in human postmortem tissue.

Confidence in these findings is strengthened by the data obtained in the autoradiography-thioflavin S double-labeling study which provides direct evidence that florbetapir F 18 labels amyloid plaques identified by thioflavin S. Further support in the findings is gained by the equivalent quantitative results obtained from three different antibodies, each binding to a different epitope of the β-amyloid peptide. Overall, these findings confirm that florbetapir F 18 is a direct and accurate marker of β-amyloid in human autopsy tissue and supports its use as a reliable marker for β-amyloid density in patients with signs and symptoms of late-life dementia.

To the best of our knowledge, this study provides the first rigorous correlation between the labeling intensity of an ^{18}F-tagged β-amyloid ligand and neuropathological measures of β-amyloid density in tissue sections from postmortem human brains. The findings are consistent with earlier data by Lockhart et al.[24] and Thompson et al.[25] who studied ^{11}C-PiB and ^{18}F-FDDNP, and Ikomovic et al.[26] who studied ^{11}C-PiB and analogs of ^{3}H-PiB, ^{18}F-FDDNP, and ^{14}C-SB13. Lockhart et al. reported high-resolution correlations between histochemically and autoradiographically demonstrated different morphological forms of β-amyloid deposition. Ikonomovic et al. reported a correlation between ^{3}H-PiB binding labeling and β-amyloid deposition quantified with an immunohistochemical method using the 6E10 β-amyloid antibody in a population of fourteen human subjects. In addition, they established a strong correlation between the binding of the fluorescent analog 6-CN-PiB and the β-amyloid immunohistochemical signal in sections from nineteen different cortical areas of a single AD subject.

The findings of this postmortem study strongly supports the conclusion that the PET signals obtained in vivo with florbetapir F 18 provide a true reflection of the overall β-amyloid aggregation in the human brain. Two small studies provide similar evidence for ^{11}C-PiB. Leinonen et al. obtained ^{11}C-PiB PET images in ten patients with intraventricular shunts and cortical biopsies.[27] Higher amyloid PET signals were seen in those patients with positive anti-Aβ immunohistochemical signals in biopsy tissue than in those without β-amyloid deposits. Burack et al. studied β-amyloid deposition postmortem in three patients with Parkinson disease dementia (PDD) who came to autopsy after ^{11}C-PiB PET imaging.[28] Two of the subjects had positive ^{11}C-PiB scans as well as abundant β-amyloid immunoreactive deposits in their brain. One subject had a negative amyloid PET scan and the brain tissue was found to have only rare β-amyloid plaques. A definitive conclusion that *in vivo* PET accurately reflects the β-amyloid brain pathology will require a prospective study, comparing amyloid PET signal intensity with postmortem β-amyloid plaque deposition. .

The current study compared florbetapir F 18 binding with estimates of total β-amyloid load in the brain using diverse methodologies including silver and thioflavin S staining, β-amyloid immunohistochemistry, and β-amyloid tissue homogenate binding. β-amyloid aggregates of different physical structures and morphologies contribute to the total β-amyloid tissue content. These include β-amyloid contained in neuritic plaques, diffuse plaques, protofibrils, soluble oligomers and less structured aggregates.[29–33] While there is no precise and generally accepted definition of the various physical forms of amyloid, all may contribute to florbetapir F 18 binding. Lockhart et al. reported correlations between histochemically- and autoradiographically-demonstrated morphological forms of amyloid deposition (including diffuse plaques, neuritic plaques, cored plaques and amyloid angiopathy).[24] These authors, as well as Ikonomovic et al.[26], also reported weak, but specific, binding of ^{11}C-PiB to neurofibrillary tangles. Due to the weakness of the signal generated by tangle binding, the authors suggested the tangle binding would not appreciably alter the overall signal when plaques are also present. The present study with florbetapir F 18 shows that there is no significant correlation between estimates of neurofibrillary tangle density and florbetapir F 18 binding in tissue sections containing both plaques and tangles.

Florbetapir F 18 holds promise as a clinically informative diagnostic tool for the evaluation of individuals with signs and symptoms of late-life cognitive impairment. The demonstration of a strong, quantitative, and statistically highly significant correlation between postmortem binding of the ligand and β-amyloid plaque deposition supports the conclusion that florbetapir F 18 binding is a reliable and quantitative marker of amyloid load in the human brain. Since the presence of β-amyloid plaques in the brain is a defining pathologic feature for Alzheimer's disease, florbetapir F 18 PET imaging of patients with signs and symptoms of progressive late-life cognitive impairment should be an informative clinical tool for the identification of AD pathology.

Acknowledgments

Financial support: This work was supported by National Institutes of Health grants (ROI-AG-022559, H.F.K., and R43AG032206, D.S.). The Rush Alzheimer's disease center is supported by the National Institute on Aging (P30 AG10161, Rush Alzheimer's Disease Core Center). The Banner Sun Health Research Institute Brain Donation Program is supported by the National Institute on Aging (P30 AG19610 Arizona Alzheimer's Disease Core Center), the Arizona Department of Health Services (contract 211002, Arizona Alzheimer's Research Center), the Arizona Biomedical Research Commission (contracts 4001, 0011, 05-901 and 1001 to the Arizona Parkinson's Disease Consortium) and the Prescott Family Initiative of the Michael J. Fox Foundation for Parkinson's Research."

Reference List

1. Recommendations to Update Diagnostic Criteria. Alzheimer's Association; 2010 Aug 8.
2. Dubois B, Feldman HH, Jacova C, et al. Research criteria for the diagnosis of Alzheimer's disease: revising the NINCDS-ADRDA criteria. Lancet Neurol. 2007; 6(8):734–746. [PubMed: 17616482]
3. Mirra SS, Heyman A, McKeel D, et al. The Consortium to Establish a Registry for Alzheimer's Disease (CERAD). Part II. Standardization of the neuropathologic assessment of Alzheimer's disease. Neurology. 1991; 41:479–486. [PubMed: 2011243]
4. Querfurth HW, LaFerla FM. Alzheimer's disease. N Engl J Med. 2010; 362(4):329–344. [PubMed: 20107219]
5. Roberson ED, Mucke L. 100 years and counting: prospects for defeating Alzheimer's disease. Science. 2006; 314(5800):781–784. [PubMed: 17082448]
6. The National Institute on Aging aRIWGoDCftNAoAD. Consensus Recommendtions for the Postmortem Diagnosis of Alzheimer's disease. Neurobiol Aging. 1997; 18(S4):1–2. [PubMed: 8983027]

7. Klunk WE, Lopresti BJ, Ikonomovic MD, et al. Binding of the positron emission tomography tracer Pittsburgh compound-B reflects the amount of amyloid-beta in Alzheimer's disease brain but not in transgenic mouse brain. J Neurosci. 2005; 25(46):10598–10606. [PubMed: 16291932]
8. Klunk WE, Mathis CA. The future of amyloid-beta imaging: a tale of radionuclides and tracer proliferation. Curr Opin Neurol. 2008; 21(6):683–687. [PubMed: 18989113]
9. Mathis CA, Wang Y, Klunk WE. Imaging beta-amyloid plaques and neurofibrillary tangles in the aging human brain. Curr Pharm Des. 2004; 10(13):1469–1492. [PubMed: 15134570]
10. Rowe CC, Ackerman U, Browne W, et al. Imaging of amyloid beta in Alzheimer's disease with 18F-BAY94-9172, a novel PET tracer: proof of mechanism. Lancet Neurol. 2008; 7(2):129–135. [PubMed: 18191617]
11. Koole M, Lewis DM, Buckley C, et al. Whole-body biodistribution and radiation dosimetry of 18F-GE067: a radioligand for in vivo brain amyloid imaging. J Nucl Med. 2009; 50(5):818–822. [PubMed: 19372469]
12. Choi SR, Golding G, Zhuang Z, et al. Preclinical properties of 18F-AV-45: a PET agent for Abeta plaques in the brain. J Nucl Med. 2009; 50(11):1887–1894. [PubMed: 19837759]
13. Zhang W, Oya S, Kung MP, Hou C, Maier DL, Kung HF. F-18 Polyethyleneglycol stilbenes as PET imaging agents targeting Abeta aggregates in the brain. Nucl Med Biol. 2005; 32(8):799–809. [PubMed: 16253804]
14. Zhang W, Kung MP, Oya S, Hou C, Kung HF. 18F-labeled styrylpyridines as PET agents for amyloid plaque imaging. Nucl Med Biol. 2007; 34(1):89–97. [PubMed: 17210465]
15. Schneidera JA, Aggarwal NT, Barnes L, Boyle P, Bennett DA. The Neuropathology of Older Persons with and Without Dementia from Community versus Clinic Cohorts. J Alzheimers Dis. 2009; 18(3):691–701. [PubMed: 19749406]
16. Beach TG, Sue LI, Walker DG, et al. The Sun Health Research Institute Brain Donation Program: description and experience, 1987–2007. Cell Tissue Bank. 2008; 9(3):229–245. [PubMed: 18347928]
17. Mirra SS, Hart MN, Terry RD. Making the diagnosis of Alzheimer's disease. A primer for practicing pathologists [see comments]. Arch Pathol Lab Med. 1993; 117:132–144. [PubMed: 8427562]
18. Walker LC, Price DL, Voytko ML, Schenk DB. Labeling of cerebral amyloid in vivo with a monoclonal antibody. J Neuropath Expl Neurol. 1994; 53(4):377–383.
19. Akiyama H, Mori H, Saido T, Kondo H, Ikeda K, McGeer PL. Occurrence of the diffuse amyloid beta-protein (Abeta) deposits with numerous Abeta-containing glial cells in the cerebral cortex of patients with Alzheimer's disease. Glia. 1999; 25(4):324–331. [PubMed: 10028915]
20. LeVine H III. Y10W beta(1–40) fluorescence reflects epitope exposure in conformers of Alzheimer's beta-peptide. Arch Biochem Biophys. 2003; 417(1):112–122. [PubMed: 12921787]
21. Grundke-Iqbal I, Iqbal K, George L, Tung YC, Kim KS, Wisniewski HM. Amyloid protein and neurofibrillary tangles coexist in the same neuron in Alzheimer disease. Proc Natl Acad Sci USA. 1989; 86(8):2853–2857. [PubMed: 2649895]
22. Wisniewski HM, Wen GY, Kim KS. Comparison of four staining methods on the detection of neuritic plaques. Acta Neuropathol. 1989; 78(1):22–27. [PubMed: 2472039]
23. Zehntner SP, Chakravarty MM, Bolovan RJ, Chan C, Bedell BJ. Synergistic tissue counterstaining and image segmentation techniques for accurate, quantitative immunohistochemistry. J Histochem Cytochem. 2008; 56(10):873–880. [PubMed: 18574255]
24. Lockhart A, Lamb JR, Osredkar T, et al. PIB is a non-specific imaging marker of amyloid-beta (Abeta) peptide-related cerebral amyloidosis. Brain. 2007; 130(Pt:10):10–15. [PubMed: 17121745]
25. Thompson PW, Ye L, Morgenstern JL, et al. Interaction of the amyloid imaging tracer FDDNP with hallmark Alzheimer's disease pathologies. J Neurochem. 2009; 109(2):623–630. [PubMed: 19226369]
26. Ikonomovic MD, Klunk WE, Abrahamson EE, et al. Post-mortem correlates of in vivo PiB-PET amyloid imaging in a typical case of Alzheimer's disease. Brain. 2008; 131(Pt:6):6–45. [PubMed: 18084012]

27. Leinonen V, Alafuzoff I, Aalto S, et al. Assessment of beta-amyloid in a frontal cortical brain biopsy specimen and by positron emission tomography with carbon 11-labeled Pittsburgh Compound B. Arch Neurol. 2008; 65(10):1304–1309. [PubMed: 18695050]
28. Burack MA, Hartlein J, Flores HP, Taylor-Reinwald L, Perlmutter JS, Cairns NJ. In vivo amyloid imaging in autopsy-confirmed Parkinson disease with dementia. Neurology. 2010; 74(1):77–84. [PubMed: 20038776]
29. Bharadwaj PR, Dubey AK, Masters CL, Martins RN, Macreadie IG. Abeta aggregation and possible implications in Alzheimer's disease pathogenesis. J Cell Mol Med. 2009; 13(3):412–421. [PubMed: 19374683]
30. Chiti F, Dobson CM. Protein misfolding, functional amyloid, and human disease. Annu Rev Biochem. 2006; 75:333–366. [PubMed: 16756495]
31. Duyckaerts C, Delatour B, Potier MC. Classification and basic pathology of Alzheimer disease. Acta Neuropathol. 2009; 118(1):5–36. [PubMed: 19381658]
32. Irvine GB, El-Agnaf OM, Shankar GM, Walsh DM. Protein aggregation in the brain: the molecular basis for Alzheimer's and Parkinson's diseases. Mol Med. 2008; 14(7–8):451–464. [PubMed: 18368143]
33. Look GC, Jerecic J, Cherbavaz DB, et al. Discovery of ADDL--targeting small molecule drugs for Alzheimer's disease. Curr Alzheimer Res. 2007; 4(5):562–567. [PubMed: 18220523]

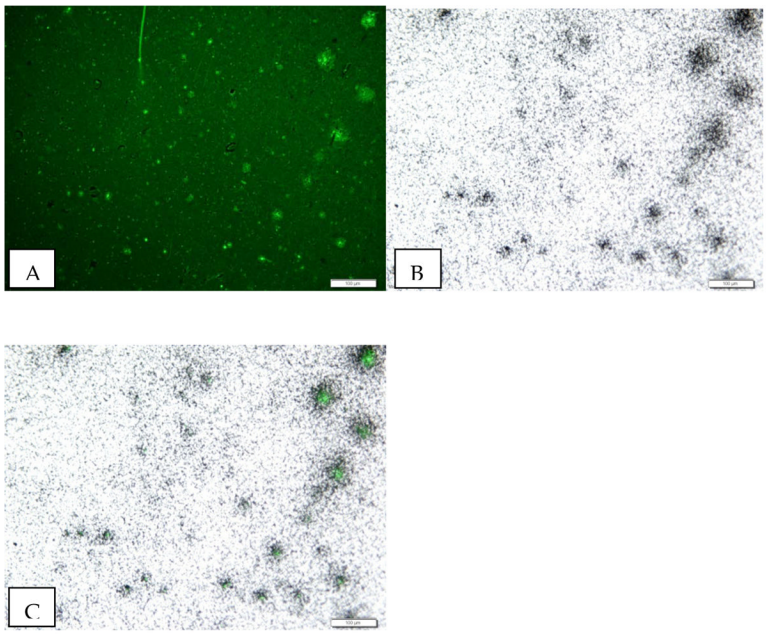

Figure 1.
Double-labeling of amyloid plaques with thioflavin S fluorescence microscopy (A) and florbetapir F 18 autoradiography (B). Image (C) shows the two figures combined. White bars indicate 100 μm.

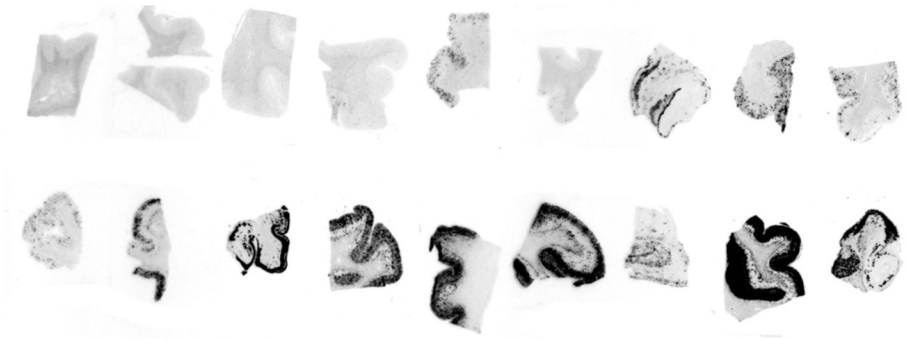

Figure 2.

In vitro florbetapir F 18. The darkly speckled band around the edge of the positive tissue sections reflects florbetapir F 18 labeling of gray matter β-amyloid, while the light central area of the tissue reflects white matter which is not specifically labeled by florbetapir F 18.

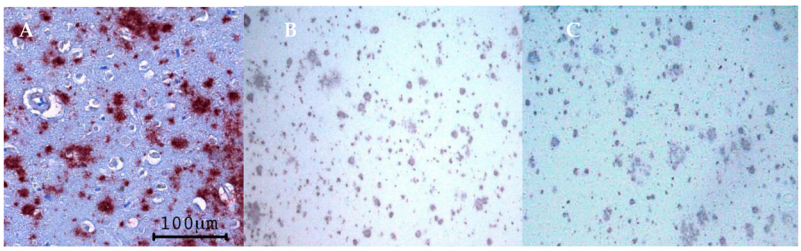

Figure 3.
Representative examples of immunohistochemical staining with 4G8 (A), 6F/3D (B), and 10D5 (C).

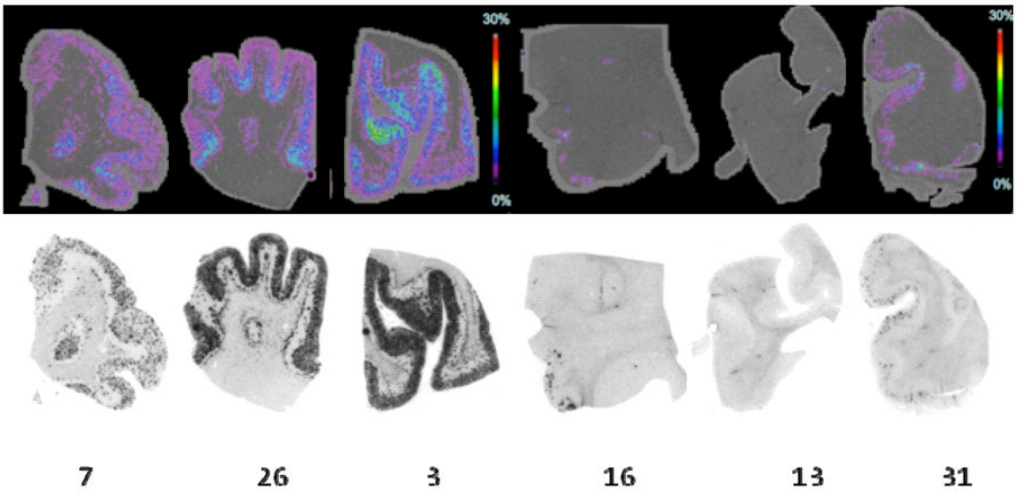

Figure 4.

Anti-Aβ immunohistochemistry with antibody 4G8 and florbetapir F 18 autoradiography on adjacent sections of human brain tissue (numbers correspond to subject numbers in Table 2-1). Top row: Parametric maps of beta-amyloid burden over the entire tissue section generated from PERMITS™ processing of digitized 4G8 IHC data. . The spectral color scale shows gray matter amyloid burden per unit area (0–30%). Bottom row: florbetapir F 18 autoradiography.

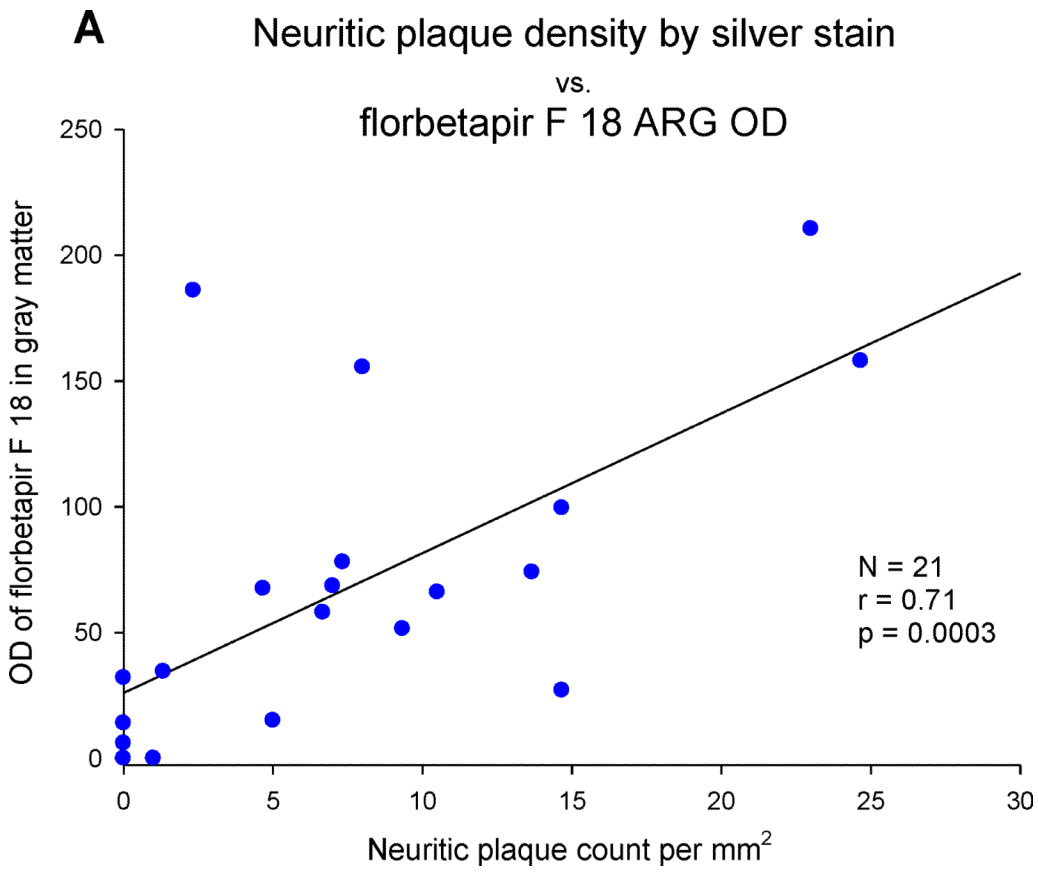

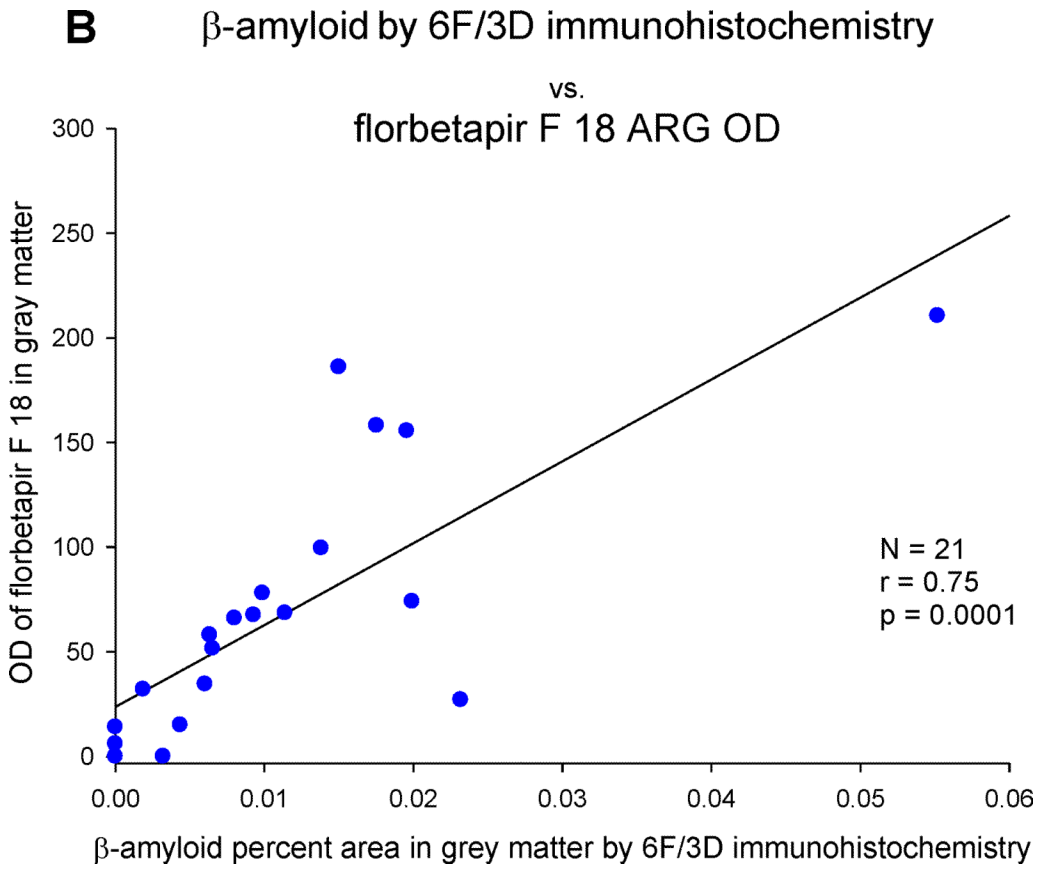

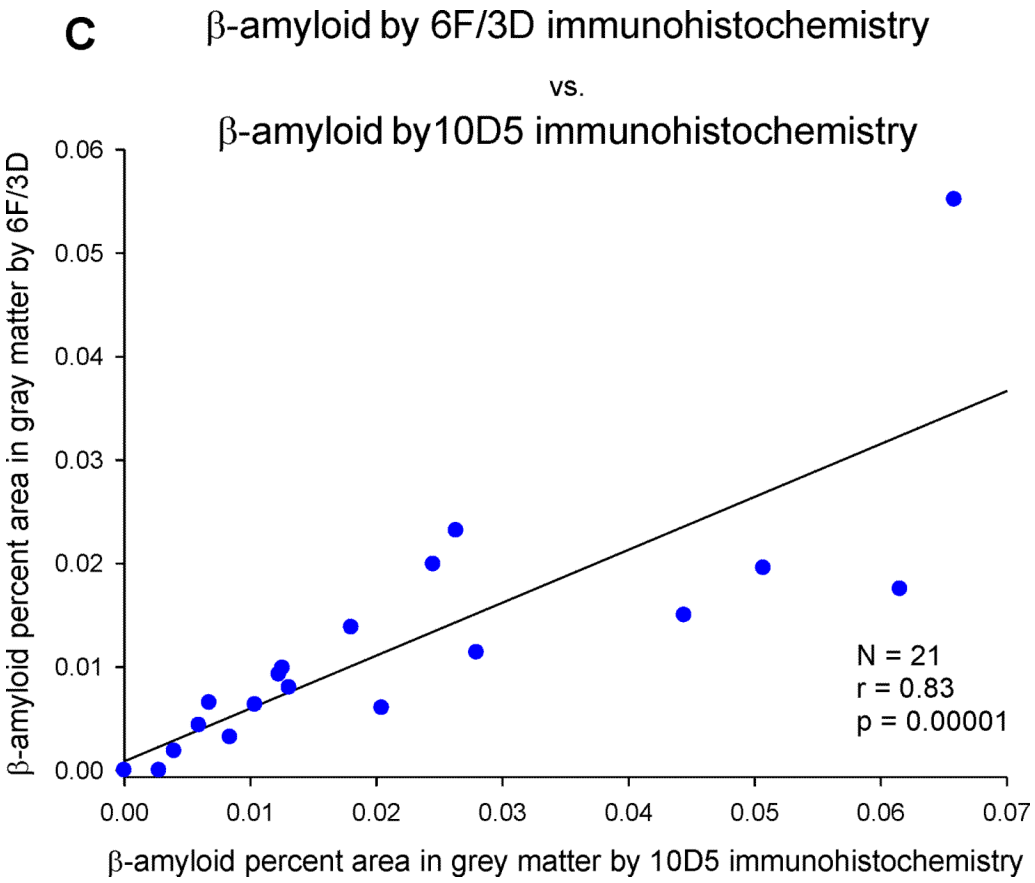

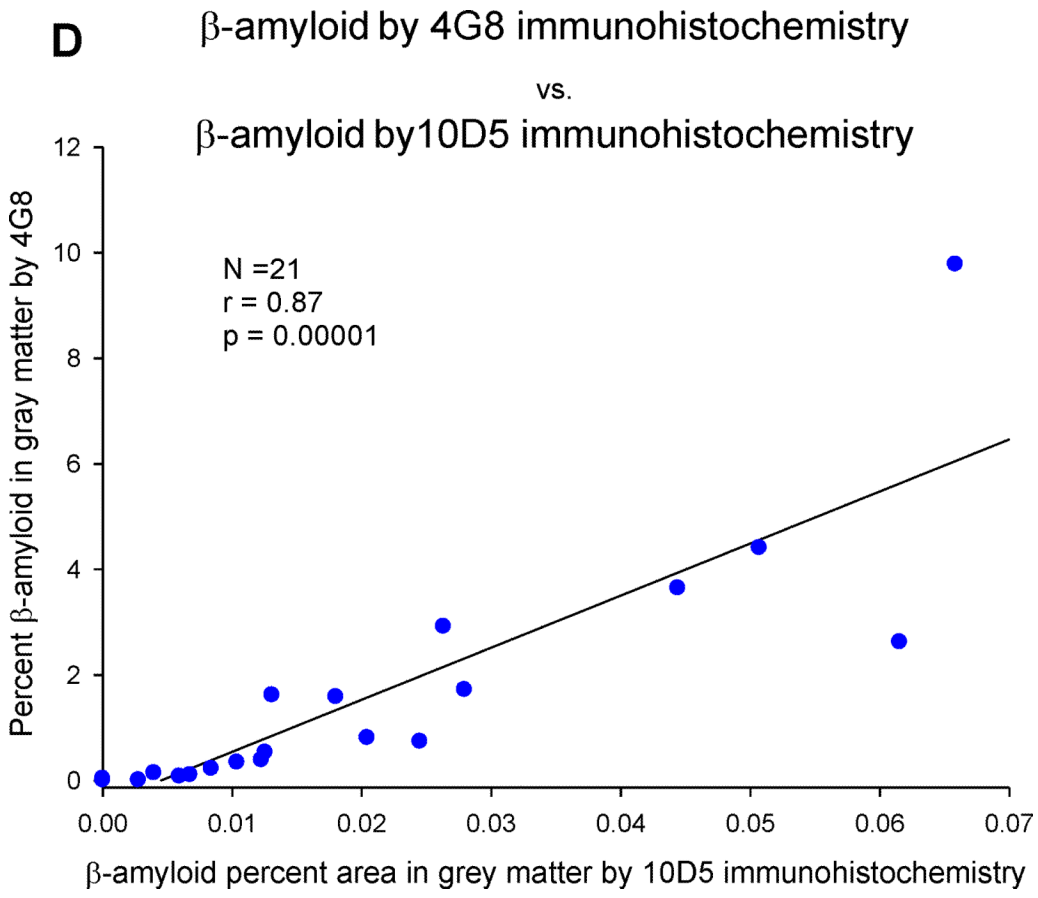

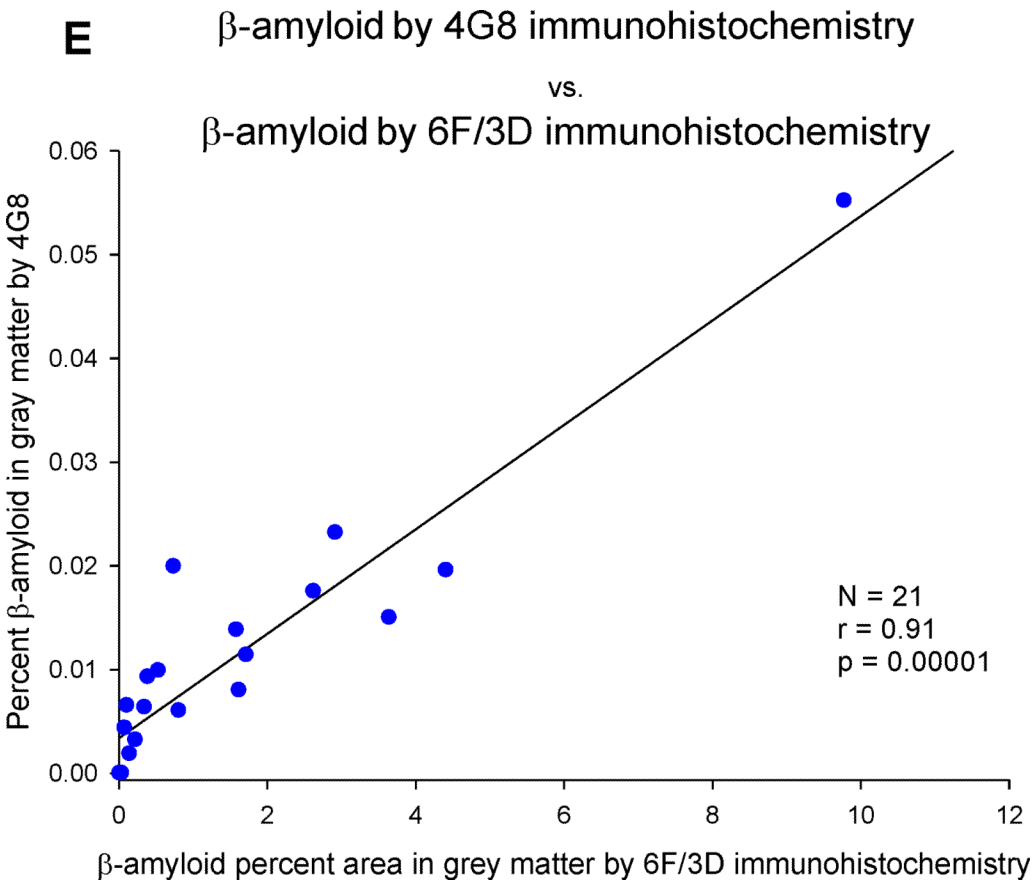

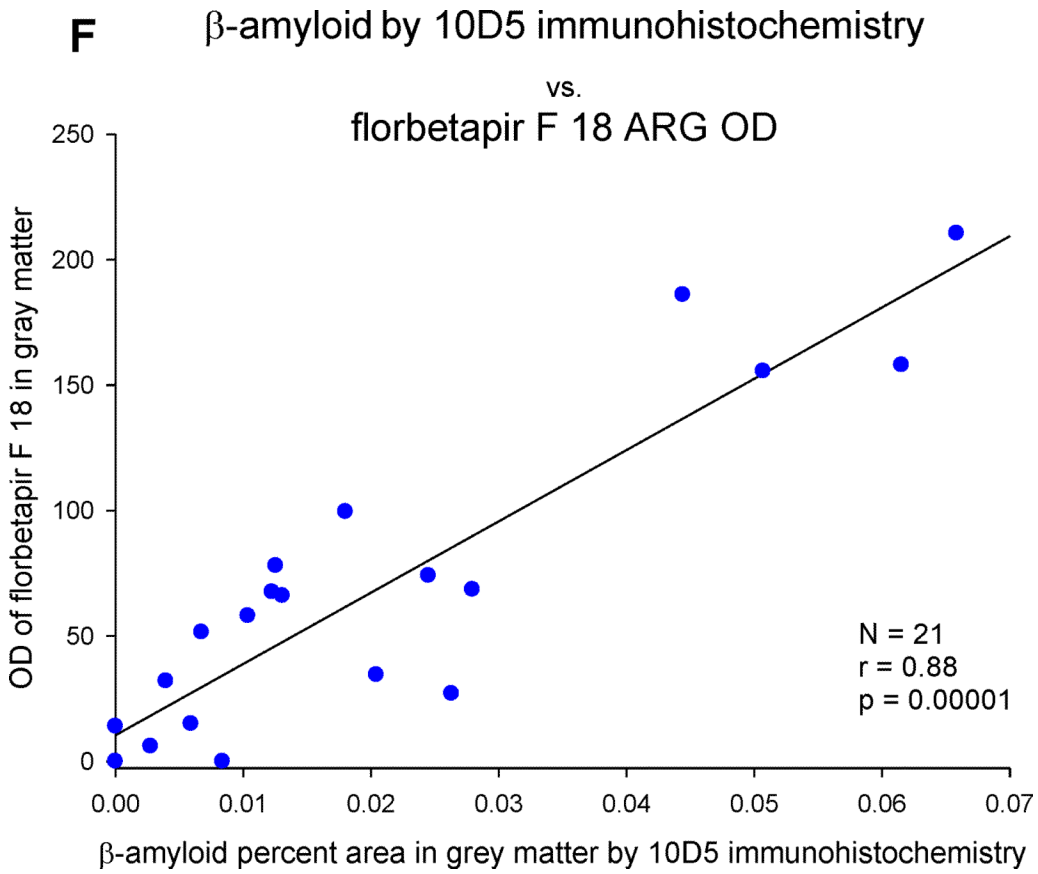

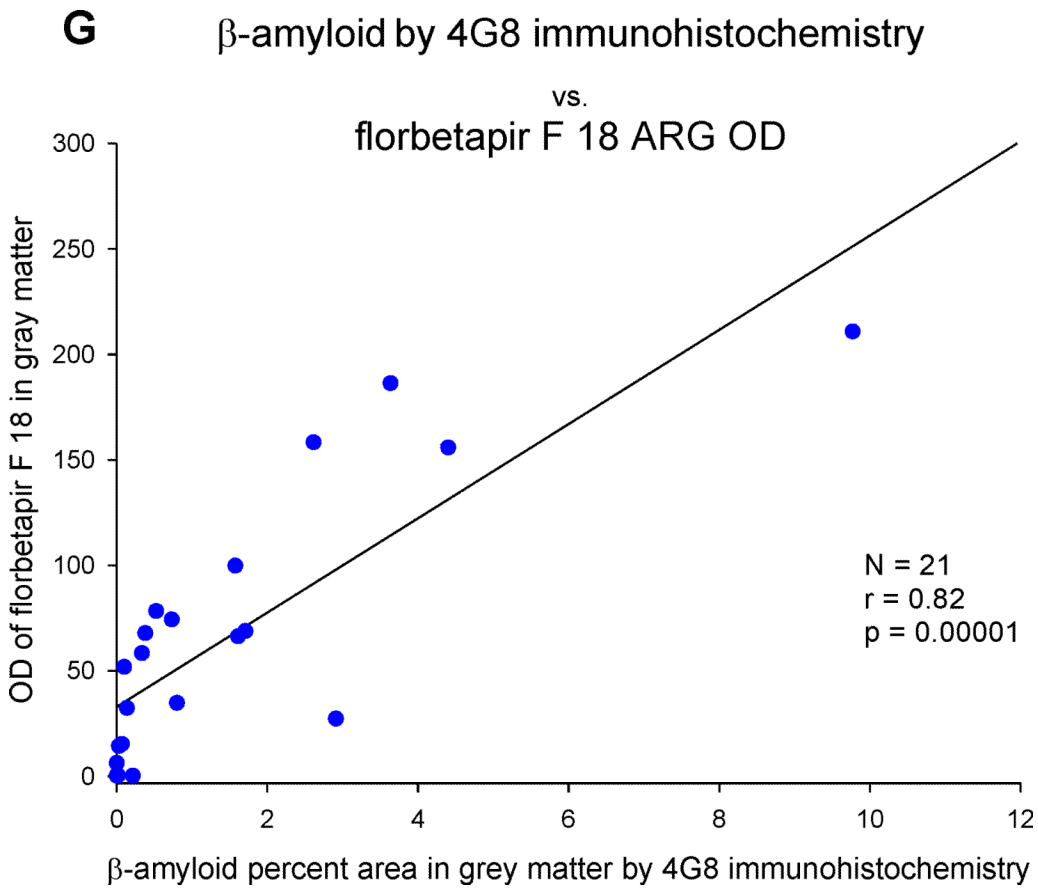

Figure 5.

(A–G): Correlations of florbetapir F 18 ARG, neuritic plaque density, and β-amyloid tissue density by immunohistochemical staining.

Table 1

Neuropathological diagnosis and florbetapir F 18 binding measures in human brain tissue

Neuropath Diagnosis & subject ID	Age/sex	Tangle score[1]	Plaque Score[1]	Florbetapir F 18 autoradiography (OD signal, n=4–5)[2]	Florbetapir F 18 binding (Bmax, n=2–7)[3]
Control1	73/M	0.0	1.0	40.5 ± 4.0	833 ± 182
Control2	84/M	0.0	1.5	84.3 ± 7.0	3213 ± 875
AD1	85/M	3.0	1.5	103.6 ± 17.8	3362 ± 524
AD2	96/F	0.0	2.5	156.8 ± 9.4	7534 ± 424
AD3	86/M	2.25	2.5	182.6 ± 4.7	9361 ± 432
AD4	78/F	1.5	3.0	191.4 ± 9.8	8966 ± 1067
AD5	85/M	0.5	3.0	193.4 ± 6.7	9104 ± 2582
AD6	86/M	0.5	3.0	224.4 ± 7.4	14099 ± 952
AD7	78/F	2.0	3.0	191.4 ± 15.5	5076 ± 1395
VAD1	89/F	0.0	0.0	34.2 ± 6.6	50 ± 10
VAD2	90/M	0.0	0.0	36.0 ± 7.0	50 ± 10
VAD3	70/M	0.0	0.25	32.8 ± 8.4	398 ± 211
PSP1	82/F	0.5	0.0	27.2 ± 5.1	50 ± 10
PSP2	85/M	1.5	0.75	67.6 ± 14.3	1774 ± 155
PSP3	79/M	0.5	2.0	70.6 ± 11.8	2382 ± 376
PSP4	93/M	0.0	3.0	187.6 ± 13.6	8538 ± 1498

Postmortem tissue from SHRI

[1]Tangle and plaque scores (0 = none to 3 = dense).

[2]OD values represent arbitrary absolute values.

[3]Bmax values are fmol/mg protein

AD=Alzheimer's disease

VAD=Vascular dementia

PSP=Progressive supranuclear palsy

Table 2

Correlation coefficients and p values for measures of florbetapir F 18 binding and scores of neuritic plaques or neurofibrillary tangles. [16 brain tissue samples]

Comparison	r	p
Plaque score vs. florbetapir F 18 ARG[1] OD[2]	0.95	< 0.0001
Plaque score vs. Bmaxfor florbetapir F 18 binding	0.88	< 0.0001
Bmax vs. florbetapir F 18 binding by ARG	0.95	< 0.0001
Tangle score vs. florbetapir F 18 ARG OD[1]	0.33	0.21
Tangle score vs. Bmax for florbetapir F 18 binding	0.20	0.45

[1] autoradiography

[2] optical density

Table 3

Correlation coefficients and p values of β-amyloid density evaluated by Bielschowsky silver staining, β-amyloid immunohistochemistry, thioflavin S fluorescence microscopy, and florbetapir F 18 autoradiography signal intensity in 22 brain tissue samples

	r	p
Florbetapir F 18 ARG[1] OD[2] vs. amyloid NP[3] score (silver stain)	0.71	0.0013
Florbetapir F 18 ARG OD vs. amyloid NP (thioflavin S)	0.81	< 0.0001
Florbetapir F 18 ARG OD vs. tangles score (silver stain)	0.31	0.1404
Florbetapir F 18 ARG OD vs. β-amyloid by 6F/3D IHC[4]	0.75	< 0.0001
Florbetapir F 18 ARG (OD) vs. 4G8 IHC	0.82	<0.0001
Florbetapir F 18 ARG OD vs. β-amyloid by 10D5 IHC[4]	0.88	< 0.0001
NP & DP[5] Silver stain vs. 6F/3D IHC[4]	0.71	< 0.0003
NP & DP Silver stain vs. 10D5 IHC[4]	0.79	< 0.0001
NP & DP Thioflavin S vs. 6F/3D	0.93	<0.00001
NP & DP Thioflavin S vs. 10D5 IHC[4]	0.86	< 0.00001
6F/3D IHC[4] vs. 10D5 IHC[4]	0.83	< 0.0001
6F/3D IHC[4] vs. 4G8 IHC[4]	0.91	<0.00001
10D5 IHC[4] vs. 4G8 IHC[4]	0.87	<0.00001

[1] autoradiography

[2] optical density

[3] Neuritic Plaque

[4] immunohistochemistry, grey matter only

[5] Diffuse Plaque

Table 4

Quantification of β-amyloid immunohistochemistry and florbetapir F 18 autoradiography optical density

Subject	florbetapir F 18 ARG[1]	4G8 IHC[3]	6F/3D IHC[3]	10D5 IHC[3]
2	32	0.15	0.19	0.40
3	186	3.65	1.50	4.44
5	6	0.01	0.00	0.00
7	66	1.62	0.80	1.31
8	155	4.41	1.96	5.07
11	99.5	1.59	1.38	1.80
12	27.0	2.92	2.32	2.36
13	0.0	0.03	0.00	0.00
14	0.0	0.01	0.00	0.00
15	51.5	0.11	0.65	0.67
16	15.0	0.08	0.44	0.59
17	14.0	0.04	0.00	0.00
19	74.0	0.74	1.99	2.45
21	58.0	0.35	0.63	1.04
22	210.5	9.78	5.52	6.58
26	158.0	2.63	1.75	6.15
29	68.5	1.72	1.14	2.79
30	78.0	0.54	0.99	1.25
31	34.5	0.81	0.60	2.04
33	0.0	0.23	0.32	0.84
43	67.5	0.39	0.93	1.23

Each value represents the average of two areas from the same frontal lobe of each subject.

[1] autoradiography

[2] optical density

[3] immunohistochemistry. gray matter only